physica status solidi a
www.pss-a.com

A Metamaterial-Plasmonic Scheme Based on a Random Metallic Network for Controlling Thermal Emission

*Jiantao Kong, Tianyi Sun, Feng Cao, Yang Li, Jiming Bao, Jinwei Gao, Xin Wang, Guofu Zhou, Chuanfei Guo, Zhifeng Ren, and Krzysztof Kempa**

Herein, it is demonstrated by calculations, simulations, and experiments that a class of random three-layer structures, each consisting of an insulator layer sandwiched between a continuous metallic film on one side and a randomly perforated metallic film on the other, strongly absorb electromagnetic radiation in a narrow band of frequencies (centered around 1 μm wavelength) and are highly reflecting for frequencies below this band. This response is shown to be similar to that of the periodic analogues of these structures, and so is the main physics: metamaterial plasmonics. It had been shown that the absorbance spectrum with these characteristics is beneficial for high efficiency thermal photovoltaic devices, and thus a random three-layer structure from this class is proposed, based on high temperature resistant materials (W and HfO_2), to be used as such a window filter of these devices.

1. Introduction

High efficiency thermal photovoltaic (TPV) devices rely on shaping the emission spectrum of the employed absorber-emitter, to match the spectral response of a photovoltaic (PV) detector.[1] This can be most efficiently achieved with photonic crystals[2] and metamaterials.[3] Such emission-shaping structures can be used as window filters, placed in-between the absorber-emitter and a PV detector. The basic problem is that absorber-emitters operate at very high temperature ($T > 100\,^{\circ}C$), which limits the range of possible structures and materials for the filters. Recently, a metamaterial, metal-insulator window filter design was proposed, consisting of a superlattice of alternating layers of tungsten and hafnium dioxide.[4] It was demonstrated that this design is optimal for a class of TPV window filters, and provided control of the thermal emission through an engineered effective dielectric response function of the superlattice, with minimal angular dependency, and strong suppression of the thermal emission in the near-infrared (IR) spectrum, crucial for high performance TPV.[4]

Here, we propose a different metamaterial window filter design, based on a structure consisting of only three layers: continuous metallic, continuous insulating, and the *randomly perforated metallic*. This random MIM (metal-insulator-metal) structure has been inspired by the studies, which demonstrated that a periodic analogue of this structure can function as a metamaterial superabsorber,[5–7] with tunable (by geometry) absorption spectrum. We demonstrate by simulations and experiment, that this structure can have a very similar response to that of the superlattice design of ref. [4], with strong absorption suppression in the near IR, and small angular dependency. We also show that this structure can be based on W and HfO_2, and thus it can work at very high temperatures encountered during the TPV operation.

It has been shown by detailed effective medium analysis, and confirmed by simulations that periodic MIM structures can strongly suppress reflection of electromagnetic waves.[5–10] In ref. [5] this superabsorbance was due to perfect impedance matching of the structure to the vacuum impedance (mechanism 1). In ref. [6] the plasmonic coupling between the perforated and the continuous layers was identified as the reason for the reflectance suppression (mechanism 2). The detailed analysis in ref. [7] showed that it was the magnetic plasmonic resonance due to induced current loops between the perforated and the continuous layers, which suppressed the reflection. It was also shown that a broad-band reflectance suppression was achieved in perforated films with an inherently broad-band response, such as the checkerboard structure.[11] This lead to a proposal for a solar photovoltaic (PV) cell, which implemented the checkerboard structure, and allowed

J. Kong, Dr. T. Sun, Prof. K. Kempa
Department of Physics
Boston College
Chestnut Hill, MA 02467, USA
E-mail: kempa@bc.edu

Dr. T. Sun, Dr. F. Cao, Prof. Z. Ren
Department of Physics and TcSUH
University of Houston
Houston, TX 77204, USA

Y. Li, Prof. J. Bao
Department of Electrical Engineering
University of Houston
Houston, TX 77204, USA

Prof. J. Gao
Institute for Advanced Materials and Guangdong Provincial Key Laboratory of Quantum Engineering and Quantum Materials, South China Normal University
Guangzhou 510006, China

Prof. X. Wang, Prof. G. Zhou
National Center for International Research on Green Optoelectronics
South China Normal University
Guangzhou 510006, China

Prof. C. Guo
Department of Materials Science and Engineering
Southern University of Science and Technology
Shenzhen, Guangdong 518055, China

The ORCID identification number(s) for the author(s) of this article can be found under https://doi.org/10.1002/pssa.201800206.

DOI: 10.1002/pssa.201800206

for ultra-thin PV absorbers.[7,12] Since the basic properties of the periodic MIM structures were describable with an effective medium model,[7] similar response (and underlying physics) is expected for random MIM structures, since the detailed in-plane structure of the layers is largely irrelevant: the effective medium approach assumes that the geometric details of the structures have dimensions much smaller than the radiation wavelength.

In this work we proceed as follows. We start by employing the effective medium picture to make a rough design of random MIM structures with spectral response similar to that in ref. [4]. Typically, this design requires refinement, if the conditions required by the effective medium picture are not satisfied. We have developed an extension of this approximation, the coherency model, and have shown its validity. After the preliminary structure design with the effective medium models (including the coherency model) is completed, we perform FDTD simulations to confirm the design. Finally, the designed structures are grown and their response measured.

2. Theoretical Models, Experimental Results and Discussions

The conventional effective medium model, such as the Maxwell-Garnett model, employs the long wavelength limit, i.e., assumes that the average perforation dimension ξ is much smaller than the radiation wavelength λ. Since our aim is to develop easily manufacturable random MIM structures, with feature dimensions of the order of microns, i.e., comparable to the wavelength corresponding to the superabsorption peak ($\lambda \approx 1\,\mu m$), the condition for the effective medium approximation is violated. In order to correct for this, we develop here a phenomenological extension of the effective medium approximation into the intermediate parameter region ($\xi \approx \lambda$). This extension provides a simple, approximate formula for the reflectance of radiation from a random or periodic MIM structure, valid for $\xi \leq \lambda$ (see Supporting Information for details).

$$R(\lambda) \sim \left| p\left(1 - e^{-\frac{\xi}{\lambda}}\right) r_{MS}(\lambda) + (1-p)\left(1 - e^{-\frac{\xi}{\lambda}}\right) r_P(\lambda) + e^{-\frac{\xi}{\lambda}} r_{EM}(\lambda) \right|^2 \quad (1)$$

where $r_{MS}(\lambda)$ is the Fresnel reflection coefficient from the structure without perforations (continuous metallic film), and $r_P(\lambda)$ is the Fresnel reflection coefficient from the structure without the perforated metal film. $r_{EM}(\lambda)$ is the reflection coefficient given by a Maxwell-Garnett model. Since in Equation (1) the complex reflection coefficients are weighted before the total reflectance $R(\lambda)$ is calculated, this procedure accounts phenomenologically for averaged coherence effects between the scattered electromagnetic waves; thus the *coherency model*. The weighting procedure uses an exponential factor $e^{-\frac{\xi}{\lambda}}$, in view of the two main, dimensional scales ξ and λ available, and the general form of the evanescent waves at flat metallic surfaces. As expected, for $\xi \ll \lambda$ Equation (1) reduces to the simple effective medium result $R(\lambda) \approx |r_{EM}(\lambda)|^2$. We have checked, by comparison with FDTD simulations and experiment that Equation (1) works well, providing a qualitative estimate of the reflectance across the intermediate region.

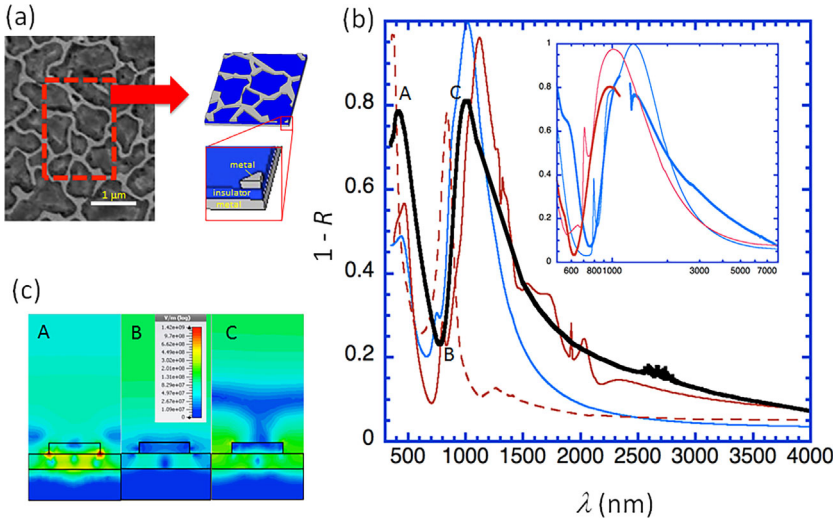

Figure 1. Structure and response spectra of random MIM structures. a) SEM image of the perforated metallic film of a designed structure. The pattern from the area of this structure outlined by a dashed rectangle was copied as a unit cell of periodically extended pattern of the structure used in calculations ($p = 0.3$) and simulation (shown immediately to the right). A fragment of this structure has been magnified to show the vertical layout. b) Absorbance spectra of this structure (Note that transmission of such MIM structure is zero). The conventional effective medium estimate based on the long wavelength model (red-dashed line), coherency model (thin-blue line) and the FDTD simulation (thin-red line). The thick-black line represents the experimental result. *The inset:* Absorbance spectra of two random Au–SiO_2 MIM structures, for two insulator thicknesses: 236 nm (blue lines) and 188 nm (red lines); thick lines (experiment); thin lines (coherency model). c) Magnitude of the electric field along a cross-section through a single line of the MIM structure at an instant of time, at three different incoming radiation wavelength marked A–C in (b). In each panel, the plane wave propagates vertically from the top to bottom, and the black lines represent edges of the metallic line, the insulator and the bottom metal. The field magnitude is color encoded, with the scale shown in the middle panel B, with zero (blue) and maximum (red).

Figure 1(a) shows the procedure used to define the MIM structure for calculations and simulations. The SEM image of the designed structure is used to extract the random pattern of the perforated layer. The pattern in the region outlined by a dashed rectangle in the image has been copied, and used as a unit cell in calculations and simulations. The specific structure shown in Figure 1(a) consists of a 35 nm thick, randomly perforated metallic film (Ag), deposited on a Ag substrate, coated with a 50 nm thick dielectric film (*a*Si). Sample preparation details can be found in the Supporting Information, as well as in refs. [13–15].

Figure 1(b) shows the absorbance spectra of this structure obtained with different calculations, simulations, and experiment. The red-dashed line in the main panel represents the conventional effective medium estimate

(based on the long wavelength model), which as discussed above is not reliable in the large frequency range due to ($\xi \approx \lambda$). The thin-solid (blue) line represents the coherency model, approximately valid in this range, and the thin-solid (red) line is the FDTD simulation, obtained by employing the CST software (*Computer Simulation Technology Microwave Studio*).[16] Unlike periodic structures, where a small unit cell can be assigned to simplify the calculation, simulations for random structures often require averaging procedures over multiple runs and on multiple areal sections, which often takes days of computation time in conventional FDTD methods. Improved, efficient FDTD codes for random systems have been developed.[17] On the other hand, simplified, much faster model calculations, have been shown to work well.[18] Our coherency model belongs to this class. Similar model solution to nonlocality problems, characterized by very computer intensive ab initio codes,[19,20] has been proposed, and shown to work well.[21]

The thick-solid line represents the measured spectrum on a sample grown according to the design. The agreement between the coherency model result, simulations, and the experiment is good; there are two pronounced maxima of absorbance (at 500 and 1000 nm), and a long tail of small absorbance for longer wavelengths, extending deep into the infrared range. We have verified by varying the geometric parameters in computation and simulation, that the mechanism 1, i.e., the near perfect impedance matching of the structure to the vacuum impedance, is responsible for the peak at the 1000 nm wavelength. In turn, it is the plasmonic coupling between the perforated and the continuous layer (mechanism 2) that is responsible for the peak at 500 nm. This is further confirmed by simulations of the magnitude of the electric field shown in Figure 1(c). The field is plotted along a cross-section through a single line of the MIM structure, for three different incoming radiation wavelength marked A–C in Figure 1(b). The field magnitude is color encoded, with the scale shown in the middle panel B, with zero (blue) and maximum (red). The maximum of the incoming wave magnitude is encoded green. Clearly at point A (peak at 500 nm) there is a large concentration of electric field in the insulator, with clear plasmonic activity in the metallic films. The corresponding movie (see Supporting Information) of the simulation of the incoming wave in this case, shows lack of standing wave, thus low reflection. This confirms the mechanism 2. The green color in the insulator at point C (1000 nm wavelength), demonstrates good penetration of field into MIM structure, but without plasmonic activity. This is consistent, and confirms the impedance matching scenario of mechanism 1, further confirmed by lack of standing wave formation outside the structure in the movie (see Supporting Information). Finally at point B, corresponding to the deep minimum at 800 nm, the penetration is suppressed (light blue color in the insulator), which leads to large reflection, further confirmed by standing wave formation in corresponding move (see Supporting Information).

The inset in Figure 1(b) shows absorbance spectra of two random MIM structures, similar to that in the main panel, but with metal changed to Au, and the insulator to SiO_2, for two dielectric thicknesses: 236 nm (blue color lines) and 188 nm (red color lines). Thick lines represent corresponding experimental results, and thin lines result from the coherency model. The spectra for these samples are almost identical to those shown in Figure 1(a) apart from small shifts, and again the coherency model represents the spectra very well.

Figure 2(a) shows spectral color maps of the absorbance for various structural parameters of these Au–SiO_2-based random MIM structures. Clearly, there is little sensitivity of the absorbance to variations of the metal film thickness, and the incident angle. On the other hand, there is strong dependency of the spectra on the insulator thickness, and the metal coverage p of the perforated structure. This confirms the plasmonic/metamaterial interpretation of the basic physics clearly identified in the earlier studies of periodic MIM structures,[6–10] and expected here as a result of the insensitivity of the coherency model to the specifics of the perforated film geometry. Overall, the main spectral features of the absorbance are similar to those in periodic MIM analogues of our structures.[22]

Figure 2(b) shows comparison of the measured absorbance spectra of the TPV metamaterial window filter design proposed in ref. [4], and coherency model calculated spectra of our W-HfO_2-based random MIM structure. The spectra overlap very well, suggesting that our structure could perform as a high performance TPV window filter. In fact, spectrum of our structure is even better suited for this application, since the most

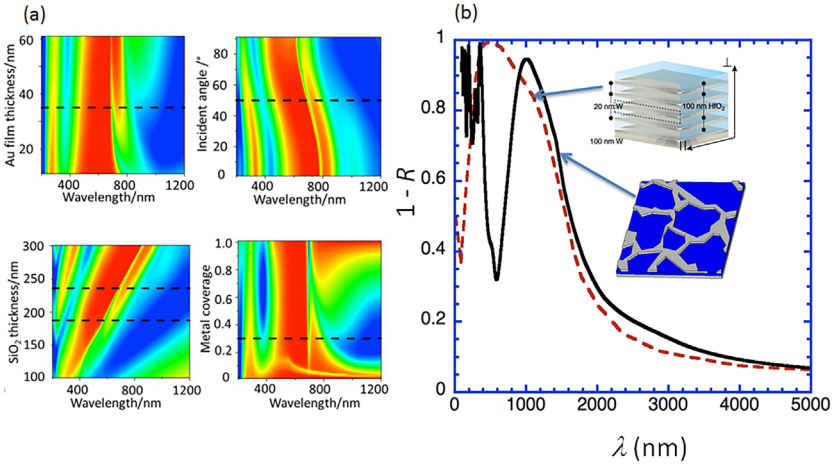

Figure 2. a) Color maps of the absorbance for various structural parameters of the Au–SiO_2-based random MIM structures. Horizontal dashed lines correspond to parameter choices used in generating curves shown in the inset of Figure 1(b). b) Comparison of the spectral response of two TPV window filters, both based on W and HfO_2. Dashed line is for the superlattice structure of ref. [4]. Inset shows a sketch of this structure. The thick-solid line represents the coherency model calculation for the random MIM structure. The corresponding inset shows a sketch of the random structure. The structure parameters are $p = 0.5$, 110 nm thickness of HfO_2, 35 nm W thickness.

important for the TPV application is the absorbance in a narrow band at $\lambda \approx 1\,\mu m$; the absorbance for shorter wavelengths is of secondary importance. Using W and HfO_2 assures high temperature operation of our structure.

3. Conclusions

In conclusion, we have studied in detail random MIM structures using calculations, simulations, and experiment. We have extended the conventional effective medium model by accounting phenomenologically for the wave coherence between scattered fields, and demonstrated its almost quantitative power in predicting the response spectra of the MIM structures. Using this coherency model, we showed that like for the periodic analogues of these structures the metamaterial plasmonics represents the basic physics, and it is behind the observed spectral features. We have also identified parameter ranges relevant for the structure design. Finally, we noticed that the characteristic spectral response of our structures is beneficial for high efficiency thermal photovoltaic devices, and thus we proposed a modification of our structure, by maximizing the peak absorbance and by switching to high-temperature resistant materials (W and HfO_2), so that it can be used as a TPV window filter for such devices.

Supporting Information

Supporting Information is available from the Wiley Online Library or from the author. See Supporting Information for fabrication of the perforated metal film, coherency model, material parameters, Maxwell-Garnett model, Fresnel optics, and videos of the propagating waves (electric field) in the simulations.

Acknowledgments

J.K. and T.S. contributed equally to this work.

Conflict of Interest

The authors declare no conflict of interest.

Keywords

metal-insulator-metal structures, metamaterials, perforated nanostructures, plasmonics, random networks, thermal photovoltaics, thin film optics

Received: March 20, 2018
Revised: April 13, 2018
Published online:

[1] C. Ferrari, F. Melino, M. Pinelli, P. R. Spina, M. Venturini, *Energy Procedia* **2014**, *45*, 160.
[2] D. L. C. Chan, M. Soljacic, J. D. Joannopoulos, *Opt. Express* **2006**, *14*, 8785.
[3] H. N. S. Krishnamoorthy, Z. Jacob, E. Narimanov, I. Kretzschmar, V. M. Menon, *Science* **2012**, *336*, 205.
[4] P. N. Dyachenko, S. Molesky, A. Y. Petrov, M. Stormer, T. Krekeler, S. Lang, M. Ritter, Z. Jacob, M. Eich, *Nat. Commun.* **2016**, *7*, 11809.
[5] X. Liu, T. Starr, A. F. Starr, W. J. Padilla, *Phys. Rev. Lett.* **2010**, *104*, 207403.
[6] J. Hao, J. Wang, X. Liu, W. J. Padilla, L. Zhou, M. Qiu, *Appl. Phys. Lett.* **2010**, *96*, 251104.
[7] Y. Wang, T. Sun, T. Paudel, Y. Zhang, Z. Ren, K. Kempa, *Nano Lett.* **2012**, *12*, 440.
[8] Q. Feng, M. Pu, C. Hu, X. Luo, *Opt. Lett.* **2012**, *37*, 2133.
[9] M. Pu, C. Hu, M. Wang, C. Huang, Z. Zhao, C. Wang, Q. Feng, X. Luo, *Opt. Express* **2011**, *19*, 17413.
[10] M. Song, H. Yu, C. Hu, M. Pu, Z. Zhang, J. Luo, X. Luo, *Opt. Express* **2013**, *21*, 32207.
[11] K. Kempa, *Phys. Status Solidi RRL* **2010**, *4*, 218.
[12] M. A. Green, S. Pillai, *Nat. Photon.* **2012**, *6*, 130.
[13] C. F Guo, Y. Lan, T. Sun, Z. Ren, *Nano Energy* **2014**, *8*, 110.
[14] C. F. Guo, T. Sun, Q. Liu, Z. Suo, Z. Ren, *Nat. Commun.* **2014**, *5*, 3121.
[15] C. F. Guo, T. Sun, Y. Wang, J. Gao, Q. Liu, K. Kempa, Z. Ren, *Small* **2013**, *9*, 2415.
[16] Computer Simulation Technology (https://www.cst.com/).
[17] M. D. Thoreson, J. Fang, A. V. Kildishev, L. J. Prokopeva, P. Nyga, U. K. Chettiar, V. M. Shalaev, V. P. Drachev, *J. Nanophoton.* **2011**, *5*, 051513.
[18] J. Y. Lu, A. Raza, N. X. Fang, G. Chen, T. Zhang, *J. Appl. Phys.* **2016**, *120*, 163103.
[19] T. V. Teperik, P. Nordlander, J. Aizpurua, A. G. Borisov, *Phys. Rev. Lett.* **2013**, *110*, 263901.
[20] P. Zhang, J. Feist, A. Rubio, P. Garcia-Gonzalez, F. J. Garcia-Vidal, *Phys. Rev. B* **2014**, *90*, 161407(R).
[21] J. Kong, A. Shvonski K. Kempa, *Phys. Rev. B* **2018**, *97*, 165423.
[22] T. Sun, E. M. Akinoglu, C. Guo, T. Paudel, J. Gao, M. Giersig, Z. F. Ren, K. Kempa, *Appl. Phys. Lett.* **2013**, *102*, 101114.